

**Supplementary information**

**Design and construction of ferrocene based inclined polycatenated Co-MOF  
for supercapacitor and dye adsorption applications**

**Richa Rajak,<sup>a</sup> Mohit Saraf,<sup>b</sup> Akbar Mohammad<sup>a</sup> and Shaikh M. Mobin<sup>\*a,b,c</sup>**

<sup>a</sup>Discipline of Chemistry, <sup>b</sup>Discipline of Metallurgy Engineering and Materials Science (MEMS) and <sup>c</sup>Centre for Biosciences and Biomedical Engineering, Indian Institute of Technology Indore, Simrol, Khandwa Road, Indore 453552, India

\*E-mail: [xray@iiti.ac.in](mailto:xray@iiti.ac.in)

Tel: +91 731 2438 762

## Contents:

**Fig. S1** XRD spectra of **1**: simulated (black), (as-synthesized (red).

**Fig. S2** XRD spectra of **2**: simulated (black), (as-synthesized (red).

**Fig. S3** TGA graph of **1**.

**Fig. S4** TGA graph of **2**.

**Fig. S5** FT-IR spectrum of **1**.

**Fig. S6** FT-IR spectrum of **2**.

**Fig. S7** SEM images of **1**.

**Fig. S8** SEM images of **2**.

**Fig. S9** Asymmetric unit of **1**.

Color code: O (red), Fe (olive), N (blue), C (dark gray), Co (magenta) and H (light gray).

**Fig. S10** Octahedral co-ordination environment around Co(II) center in **1**.

Color code: Co (magenta), N (blue), O (red).

**Fig. S11** 1D chain along *c* axis in **1**.

Color code: O (red), Fe (olive), N (blue), C (dark gray) and Co (magenta).

**Fig. S12** Space fill model of the 2D Framework showing the arrangements of FcDCA and bpy ligands along *c*-axis in **1**.

**Fig. S13** (a) Inter/Intra-molecular H- bonding Interaction between the two 2D frameworks, and (b) Packing diagram of **1** showing a 3D framework formed *via* inter/intra-molecular hydrogen-bonding and  $\pi$ – $\pi$  interaction (blue:  $\pi$ ... $\pi$ ; green: H-bonding).

**Fig. S14**. Pentagonal bipyramidal co-ordination environment around Co(II) center in **2**. Color code: Co (magenta), N (blue), O (red).

**Table S1.** Bond lengths [ $\text{\AA}$ ] and angles [ $^\circ$ ] for **1**.

**Table S2.** H-bonding Interactions in **1**.

**Fig. S15** (a) CV profiles of **2-GCE** at varied scan rates (10-500 mV  $\text{s}^{-1}$ ), (b) GCD curves for **2-GCE** at varied current densities (1.2-50 A  $\text{g}^{-1}$ ), and (c) GCD curves for **2-GCE** at 1.2 A  $\text{g}^{-1}$ , in 1 M KOH solution.

**Fig. S16** (a) Comparison of CV profiles of **1-GCE** and **2-GCE** at a scan rate of 100 mV  $\text{s}^{-1}$ , (b) comparison of GCD profiles of **1-GCE** and **2-GCE** at 1.2 A  $\text{g}^{-1}$ .

**Fig. S17** Comparison of CV profiles of **1-GCE** before and after cycling.

**Fig. S18**  $\text{N}_2$  isotherm and BJH plot of (a) **1** and (b) **2**, respectively.

**Fig. S19** AC conductivity test of **1** and **2**.

**Fig. S20** Adsorption of CSB and CR on **1**.

**Fig. S21** Color change of the reaction system containing (A) CSB, (B) CR in water on **1**.

**Fig. S22** Color change of **1**, (A) before adsorption, (B) after adsorption of CSB (C) after adsorption of CR.

**Fig. S23** UV-vis spectra of aqueous solution of CSB adsorption by **2**.

**Fig. S24** UV-vis spectra of aqueous solution of CR adsorption by **2**.

**Fig. S25** FTIR analysis of CSB adsorbed on **1** (**CSB@1**).

**Fig. S26** FTIR analysis of CR adsorbed on **1** (**CR@1**).

**Fig. S27** Recyclability study of **1** towards (a) CSB and (b) CR.

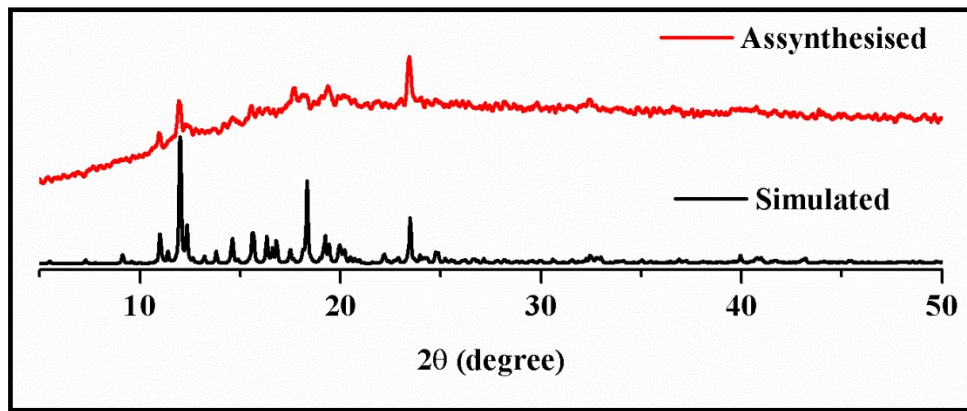


**Fig. S1** XRD spectra of **1**: simulated (black), (as-synthesized (red)).

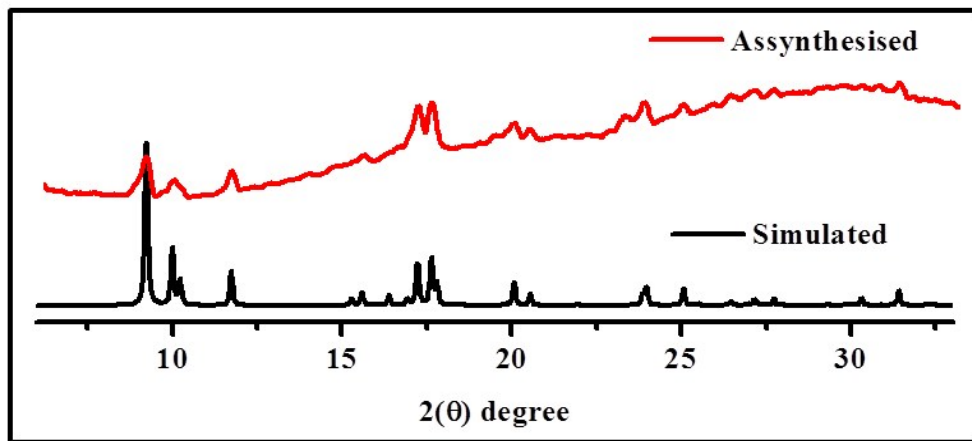


**Fig. S2** XRD spectra of **2**: simulated (black), (as-synthesized (red)).

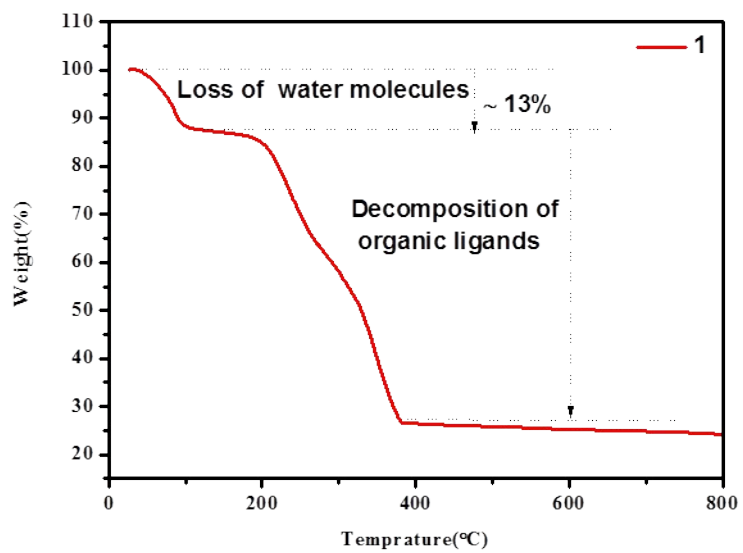


Fig. S3 TGA graph of 1.

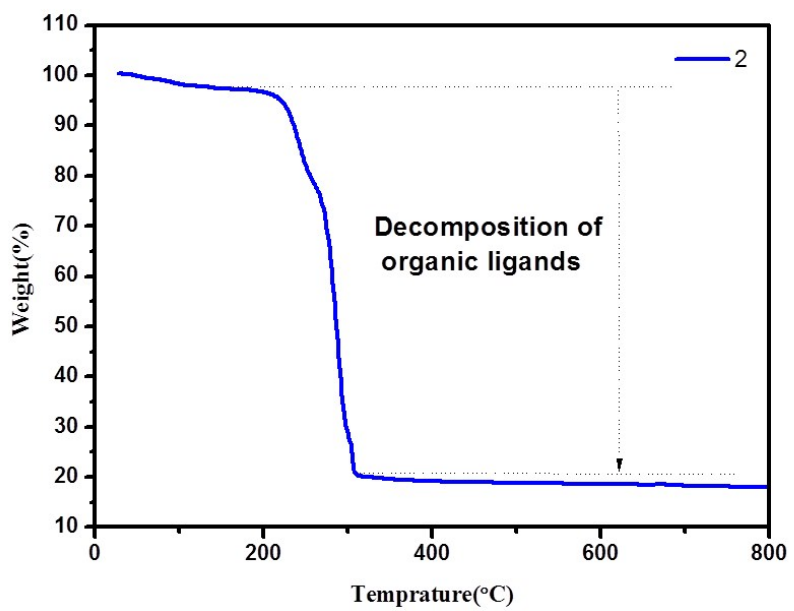
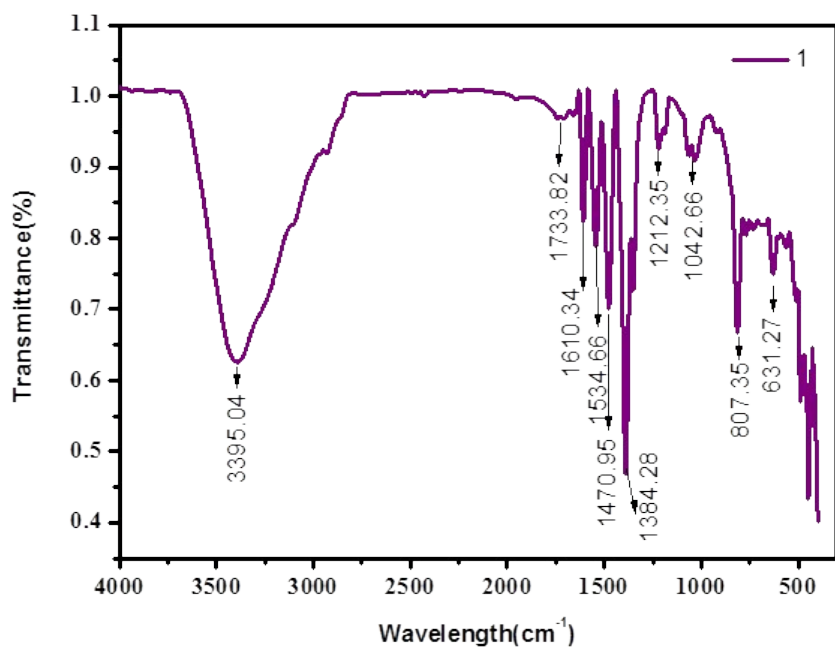
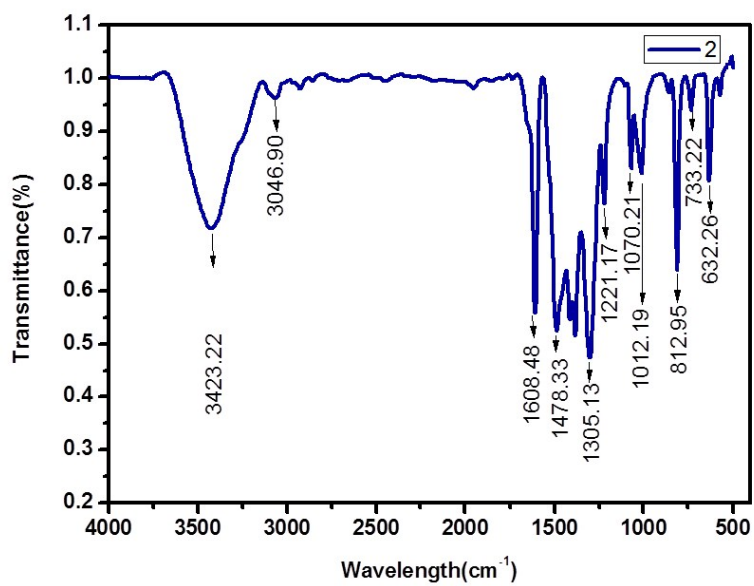


Fig. S4 TGA graph of 2.



**Fig. S5** FT-IR spectrum of **1**.



**Fig. S6** FT-IR spectrum of **2**.

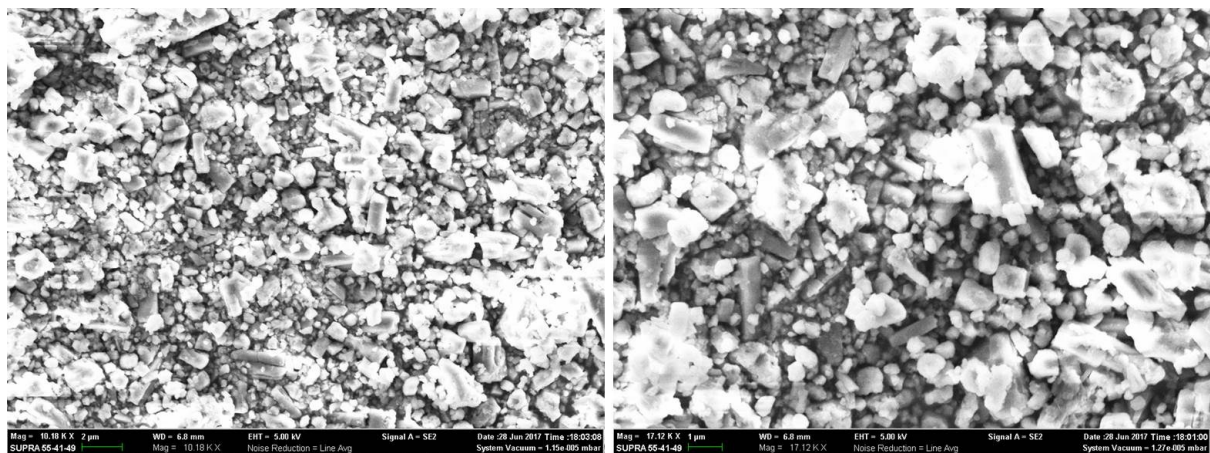
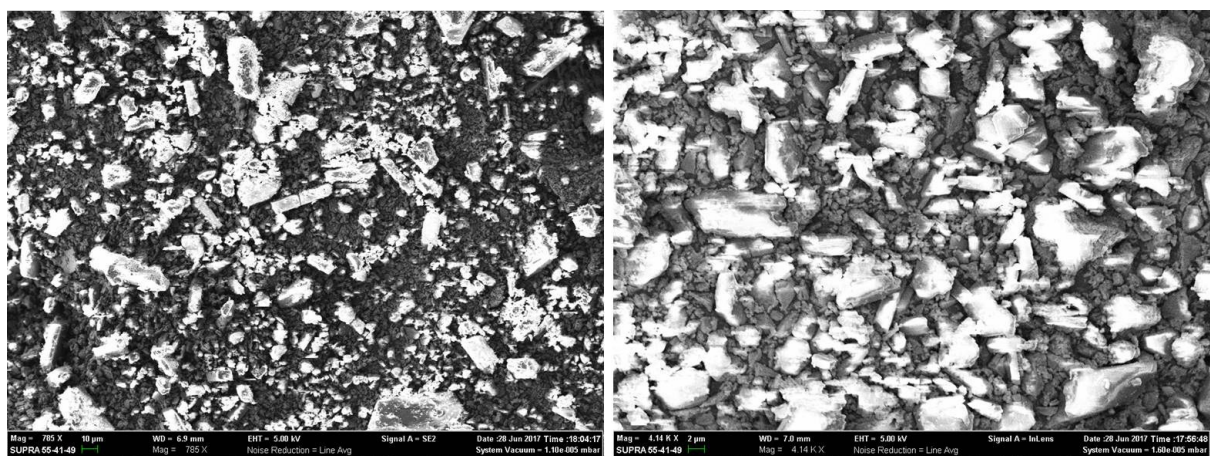
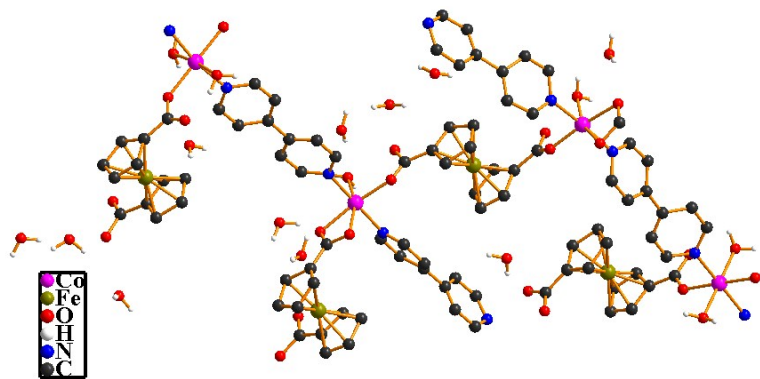


Fig. S7 SEM images of 1.





**Fig. S9** Asymmetric unit of **1**.

Color code: O (red), Fe (olive), N (blue), C (dark gray), Co (magenta) and H (light gray).

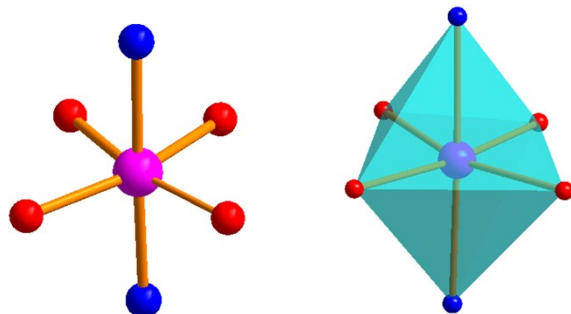


**Fig. S10** Octahedral co-ordination environment around Co(II) center in **1**.

Color code: Co (magenta), N (blue), O (red).

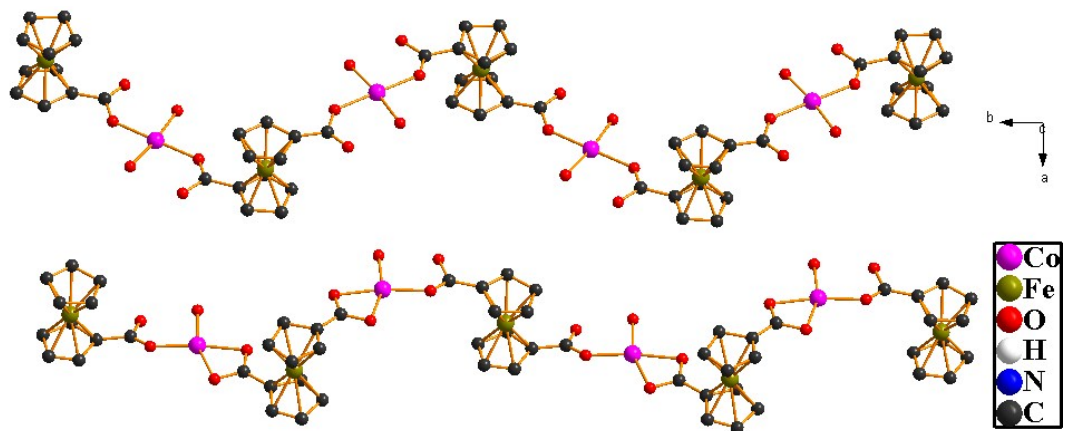


**Fig. S11** 1D chain along *c* axis in **1**.

Color code: O (red), Fe (olive), N (blue), C (dark gray) and Co (magenta).

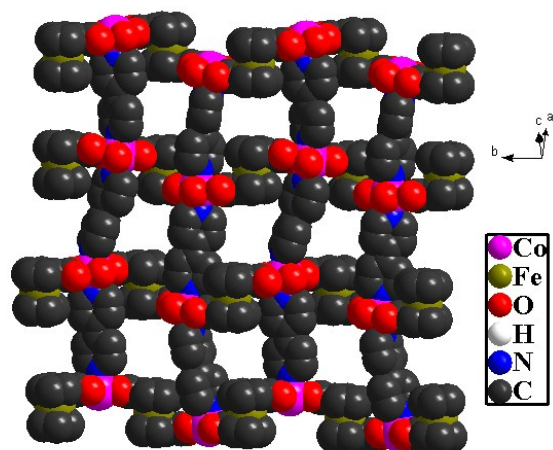


**Fig. S12** Space fill model of the 2D Framework showing the arrangements of FcDCA and bpy ligands along *c*-axis in **1**.

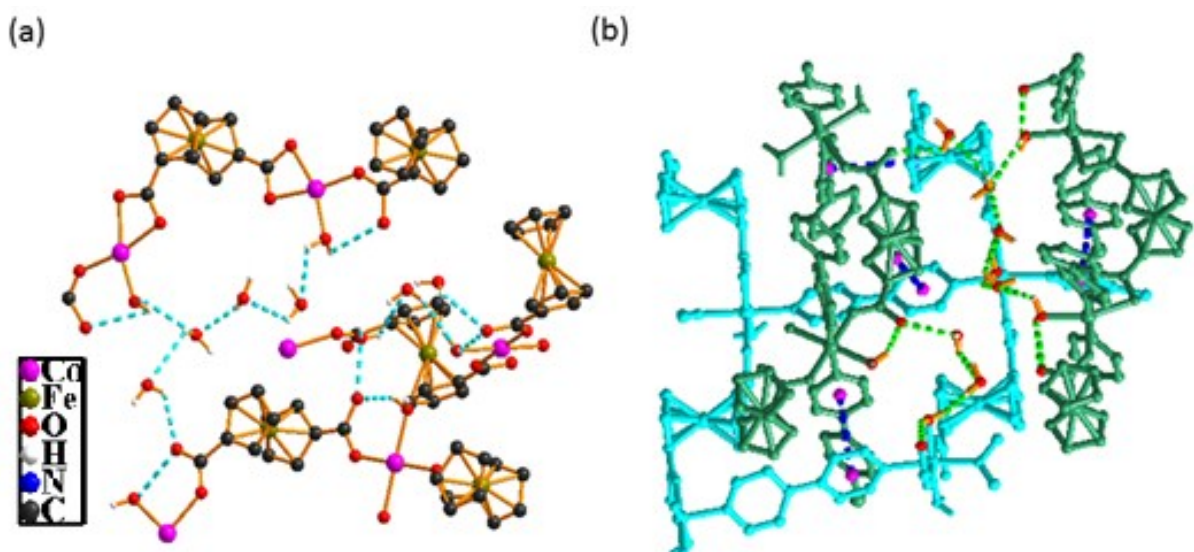


**Fig. S13** (a) Inter/Intra-molecular H- bonding Interaction between the two 2D frameworks, and (b) Packing diagram of **1** showing a 3D framework formed *via* inter/intra-molecular hydrogen-bonding and  $\pi\ldots\pi$  interaction (blue:  $\pi\ldots\pi$ ; green: H-bonding).

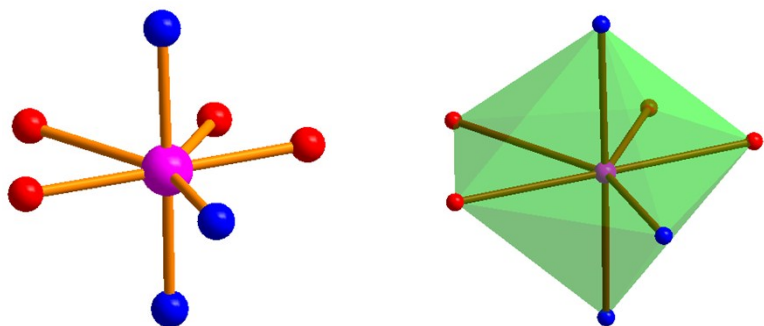


**Fig. S14.** Pentagonal bipyramidal co-ordination environment around Co(II) center in **2**. Color code: Co (magenta), N (blue), O (red).

**Table S1.** Bond lengths [Å] and angles [°] for **1**.

Bond distances	
Co(1) —O(4)#1	2.07(2)
Co(1) —O(1)	2.106(18)
Co(1) —O(5)	2.12(2)
Co(1) —O(6)	2.12(2)
Co(1) —N(1)	2.15(2)
Co(1) —N(6)#1	2.19(2)
Co(2) —O(7)	1.99(2)
Co(2) —O	2.067(18)
Co(2) —N(3)	2.11(2)
Co(2) —O(20)#2	2.122(19)
Co(2) —N(2)	2.12(2)
Co(2) —O(21)#2	2.19(2)
Co(3) —O(10)	2.03(2)
Co(3) —O(17)	2.091(19)
Co(3) —O(18)	2.11(2)
Co(3) —N(7)	2.16(2)
Co(3) —N(5)	2.18(2)
Co(3) —O(19)	2.18(2)
Co(4) —O(11)	2.080(18)
Co(4) —O(16)#3	2.080(19)
Co(4) —O(13)	2.087(18)
Co(4) —O(12)	2.103(18)
Co(4) —N(8)	2.13(2)
Co(4) —N(4)#4	2.19(2)
Bond angles	
O(4)#1—Co(1) —O(1)	178.7(9)
O(4)#1—Co(1) —O(5)	93.2(10)
O(1) —Co(1) —O(5)	86.9(9)
O(4)#1—Co(1) —O(6)	87.6(9)
O(1) —Co(1) —O(6)	92.3(8)
O(5) —Co(1) —O(6)	179.1(10)
O(4)#1—Co(1) —N(1)	91.6(10)
O(1) —Co(1) —N(1)	89.7(9)
O(5) —Co(1) —N(1)	90.2(10)
O(6) —Co(1) —N(1)	90.0(11)
O(4)#1—Co(1) —N(6)#1	87.5(9)
O(1) —Co(1) —N(6)#1	91.2(9)
O(5) —Co(1) —N(6)#1	88.2(8)
O(6) —Co(1) —N(6)#1	91.6(9)
N(1) —Co(1) —N(6)#1	178.1(10)
O(7) —Co(2) —O(22)	90.4(8)
O(7) —Co(2) —N(3)	87.8(10)
O(22) —Co(2) —N(3)	88.3(10)
O(7) —Co(2) —O(20)#2	170.9(9)
O(22) —Co(2) —O(20)#2	98.6(9)

N(3) —Co(2) —O(20)#2	93.5(10)
O(7) —Co(2) —N(2)	89.2(8)
O(22) —Co(2) —N(2)	94.3(9)
N(3) —Co(2) —N(2)	176.0(11)
O(20)#2—Co(2) —N(2)	89.2(8)
O(7) —Co(2) —O(21)#2	109.5(9)
O(22) —Co(2) —O(21)#2	160.1(9)
N(3) —Co(2) —O(21)#2	92.0(9)
O(20)#2—Co(2) —O(21)#2	61.5(8)
N(2) —Co(2) —O(21)#2	86.6(9)
O(10) —Co(3) —O(17)	93.7(9)
O(10) —Co(3) —O(18)	167.3(9)
O(17) —Co(3) —O(18)	99.0(9)
O(10) —Co(3) —N(7)	89.4(8)
O(17) —Co(3) —N(7)	89.9(9)
O(18) —Co(3) —N(7)	90.3(9)
O(10) —Co(3) —N(5)	90.1(10)
O(17) —Co(3) —N(5)	92.0(9)
O(18) —Co(3) —N(5)	89.8(10)
N(7) —Co(3) —N(5)	178.1(11)
O(10) —Co(3) —O(19)	104.7(9)
O(17) —Co(3) —O(19)	161.3(9)
O(18) —Co(3) —O(19)	62.6(8)
N(7) —Co(3) —O(19)	87.0(8)
N(5) —Co(3) —O(19)	91.3(9)
O(10) —Co(3) —C(77)	136.2(12)
O(17) —Co(3) —C(77)	130.0(12)
O(18) —Co(3) —C(77)	31.1(9)
N(7) —Co(3) —C(77)	88.4(9)
N(5) —Co(3) —C(77)	90.7(10)
O(19) —Co(3) —C(77)	31.6(9)
O(11) —Co(4) —O(16)#3	93.1(8)
O(11) —Co(4) —O(13)	87.8(8)
O(16)#3—Co(4) —O(13)	179.1(9)
O(11) —Co(4) —O(12)	173.7(8)
O(16)#3—Co(4) —O(12)	92.6(8)
O(13) —Co(4) —O(12)	86.5(9)
O(11) —Co(4) —N(8)	90.6(9)
O(16)#3—Co(4) —N(8)	87.9(9)
O(13) —Co(4) —N(8)	92.2(8)
O(12) —Co(4) —N(8)	87.0(9)
O(11) —Co(4) —N(4)#4	92.7(10)
O(16)#3—Co(4) —N(4)#4	83.5(9)
O(13) —Co(4) —N(4)#4	96.3(8)
O(12) —Co(4) —N(4)#4	90.5(9)
N(8) —Co(4) —N(4)#4	170.9(10)

Symmetry transformations used to generate equivalent atoms:

#1 -x+2,y-1/2,-z+3/2 #2 x,y-1,z #3 -x,y-1/2,-z+1/2

#4 -x,y+1/2,-z+1/2

**Table S2.** H-bonding Interactions in **1**.

D-H····A	D-H	H···A	D···A	$\angle$ D-H···A
O12-H12B···O14 (0)	0.938	1.699	2.567(.030)	152.42
O110-H11C···O111 (18)	0.938	1.976	2.791(.018)	144.13
O107-H10M···O103 (11)	0.938	2.469	2.805(.023)	103.10
O106-H10L···O109 (11)	0.938	2.077	2.712(.017)	123.69
O105-H10J···O102 (8)	0.938	2.320	2.822(.019)	113.08
O109-H10R···O106 (5)	0.938	1.963	2.712(.017)	135.46
O102-H10C···O107 (5)	0.938	2.077	2.786(.015)	131.19
O17-H17B···O107 (5)	0.938	2.143	2.805(.023)	126.55
O11-H11B···O15 (3)	0.938	1.815	2.625(.030)	142.90
O103-H10E···O107 (5)	0.938	2.627	2.948(.017)	100.64
O5-H5B···O3 (2)	0.938	1.816	2.657(.033)	147.79
O5-H5A···O108 (1)	0.938	2.375	2.931(.027)	117.68
O110-H11D···O106 (0)	0.938	2.015	2.581(.017)	117.10
O106-H10K···O110 (0)	0.938	2.096	2.581(.017)	110.73
O103-H10F···O104 (0)	0.938	2.481	2.854(.013)	103.82
O102-H10D···O101 (0)	0.938	2.088	2.612(.014)	113.79
O22-H22A···O105 (0)	0.938	2.317	2.728(.026)	105.95
O107-H10M···O17 (11)	0.938	2.469	2.805(.023)	101.10
O111-H11F···O110 (14)	0.938	2.385	2.791(.018)	105.87
O103-H10E···O2 (16)	0.938	2.327	2.749(.024)	106.81
O103-H10F···O104 (0)	0.938	2.481	2.854(.013)	103.82
O101-H10A···O18 (0)	0.938	2.449	2.805(.023)	102.42

Equivalent positions:

- (0) x,y,z
- (1) -x+1/2+1,-y+1,+z+1/2
- (2) -x+2,+y-1/2,-z+1/2+1
- (3) -x,+y-1/2,-z+1/2
- (4) -x+1/2,-y,+z-1/2
- (5) -x+1/2,-y+1,+z+1/2
- (8) x,+y-1,+z
- (11) -x+1/2,-y+1,+z-1/2
- (14) x+1/2,-y+1/2+1,-z+1
- (16) -x+1,+y+1/2,-z+1/2+1
- (18) x-1/2,-y+1/2+1,-z+1

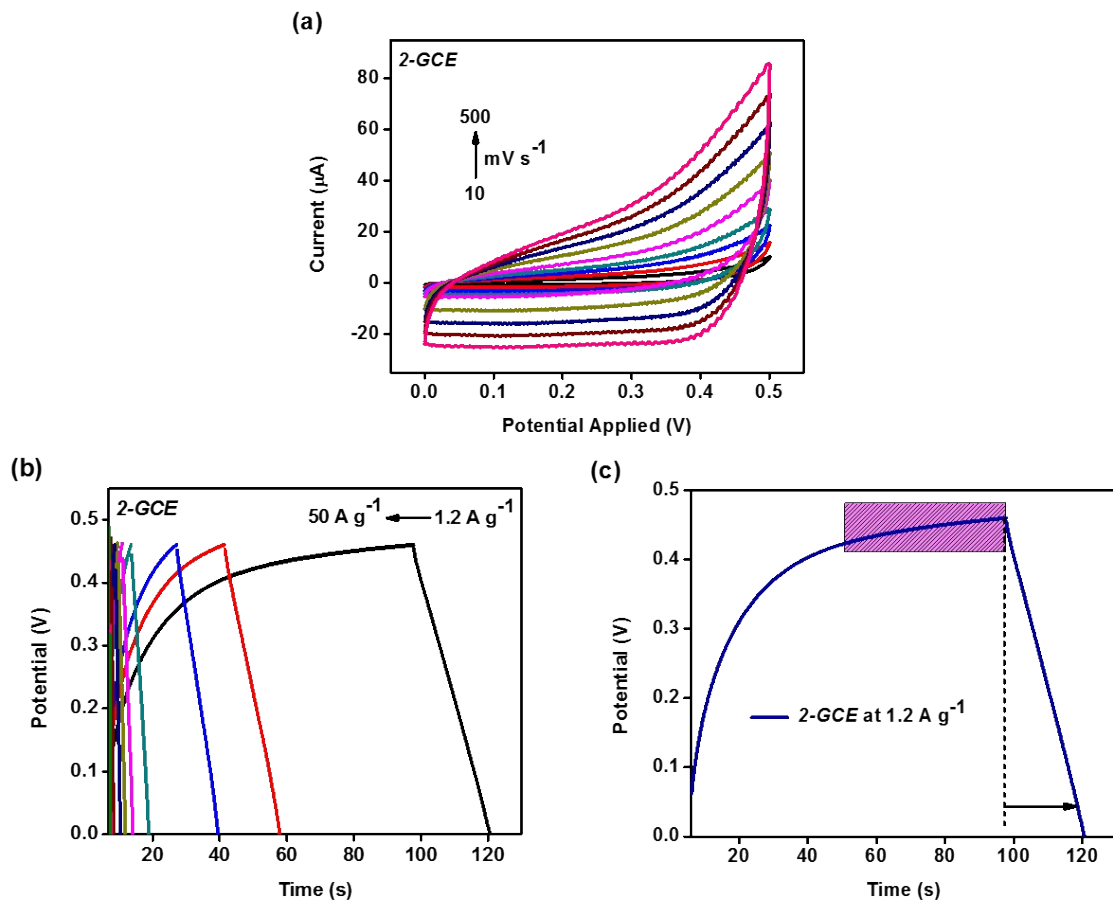


**Fig. S15** (a) CV profiles of **2-GCE** at varied scan rates ( $10\text{-}500\text{ mV s}^{-1}$ ), (b) GCD curves for **2-GCE** at varied current densities ( $1.2\text{-}50\text{ A g}^{-1}$ ), and (c) GCD curves for **2-GCE** at  $1.2\text{ A g}^{-1}$ , in  $1\text{ M KOH}$  solution.

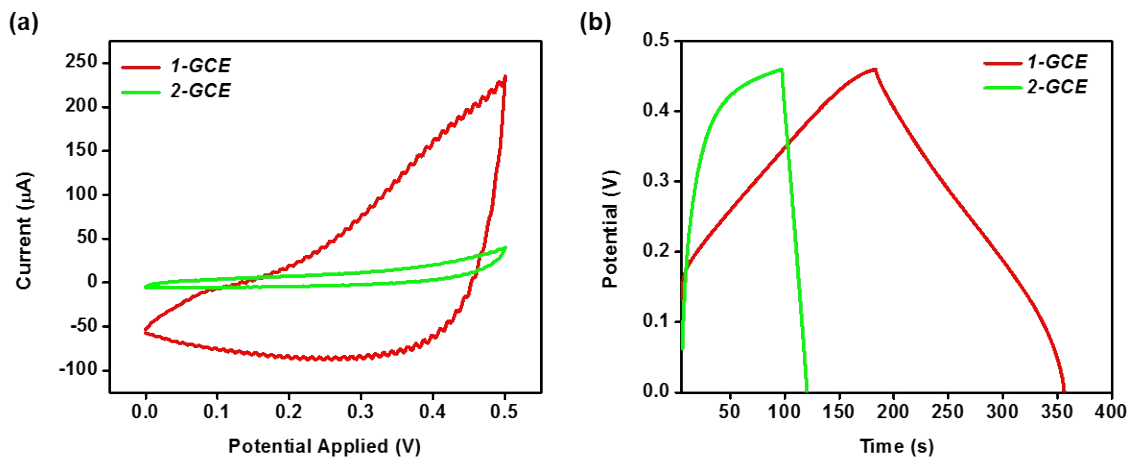


**Fig. S16** (a) Comparison of CV profiles of **1-GCE** and **2-GCE** at a scan rate of  $100 \text{ mV s}^{-1}$ , (b) comparison of GCD profiles of **1-GCE** and **2-GCE** at  $1.2 \text{ A g}^{-1}$ .

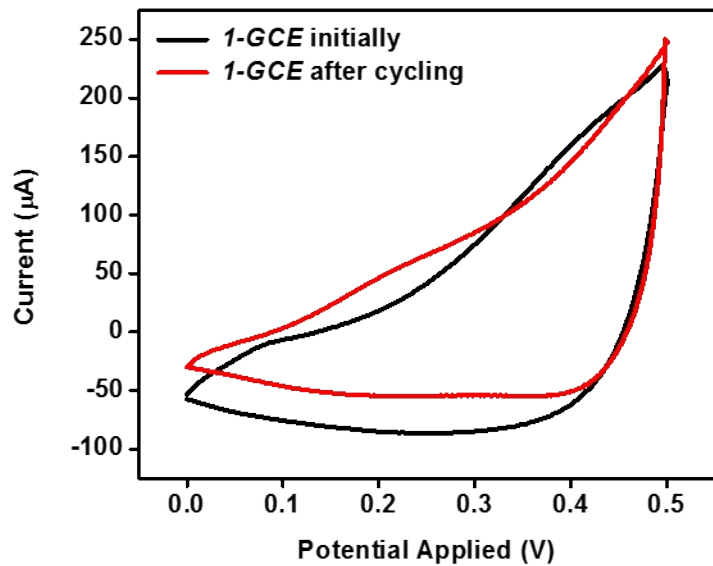


**Fig. S17** Comparison of CV profiles of **1-GCE** before and after cycling.

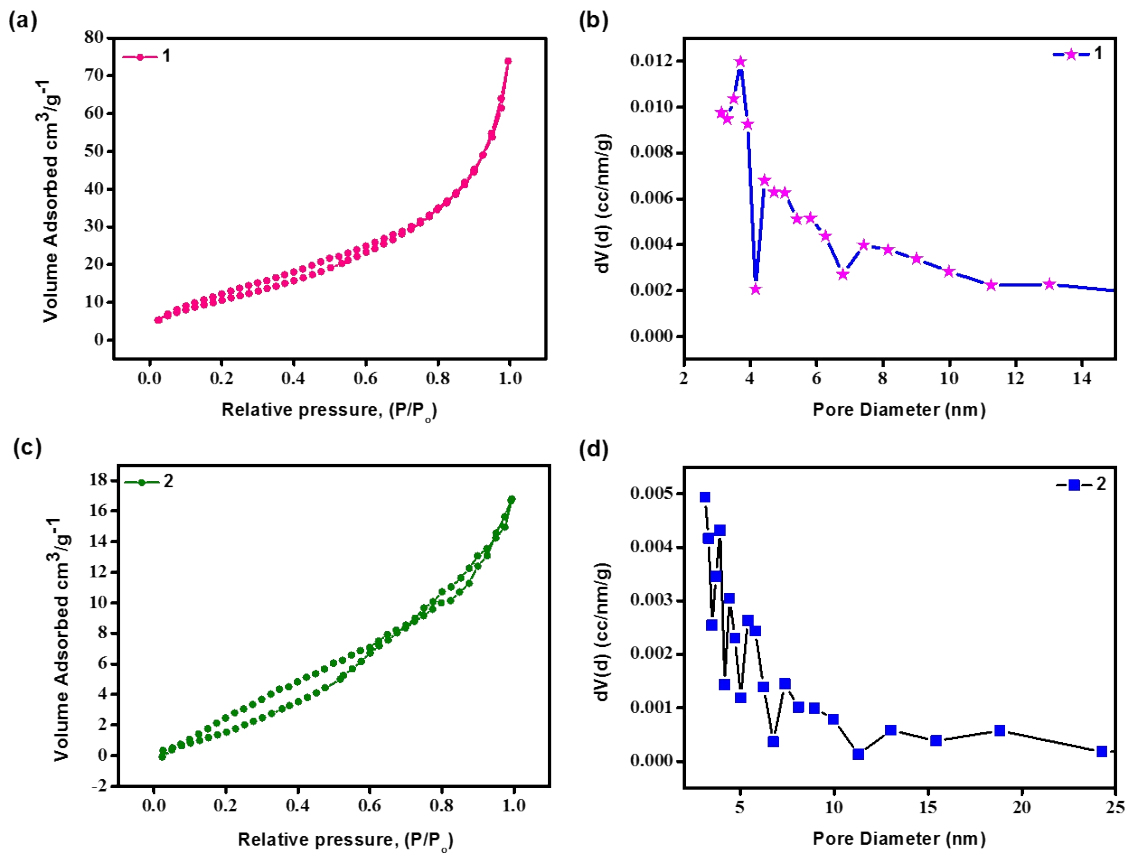


**Fig. S18**  $N_2$  isotherm and BJH plot of (a) **1** and (b) **2**, respectively.

The  $N_2$  isotherm reveals a high BET surface area of  $41.56 \text{ m}^2/\text{g}$  for **1** and  $10.306 \text{ m}^2/\text{g}$  for **2** as obtained from Fig. S18a and Fig. S18c, respectively. Additionally, the BJH curves have also been shown for **1** and **2** in Fig. S18b and Fig. S18d, respectively.

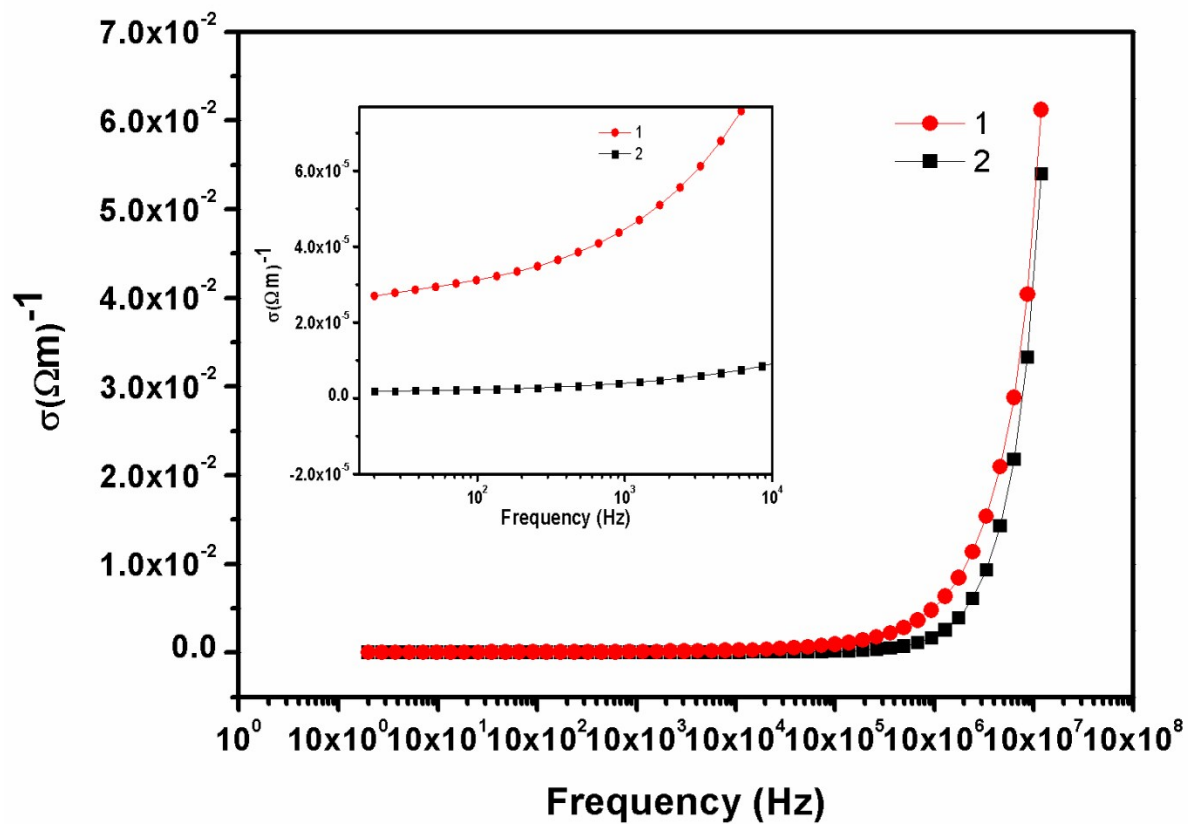


**Fig. S19** AC conductivity test of **1** and **2**.

The AC conductivity measurements were performed to reveal the conductivity of **1** and **2**. The resistance of **1** and **2** were analysed with varying frequencies and the conductivities were plotted as shown in **Fig. S19**. The results clearly show that **1** has better conductivity than **2**.

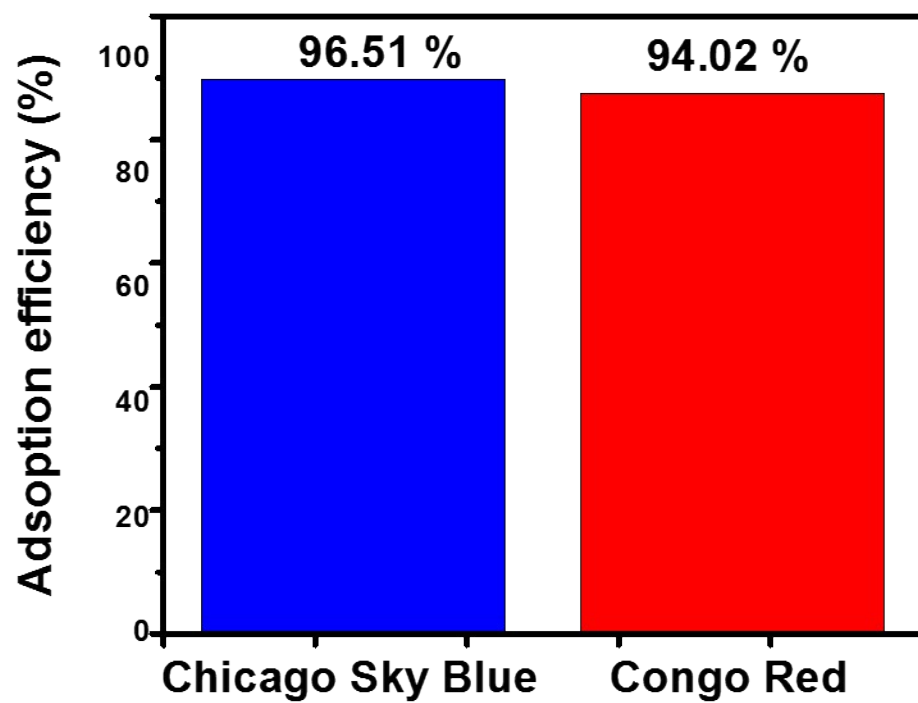


**Fig. S20** Adsorption of CSB and CR on **1**.



**Fig. S21** Color change of the reaction system containing (A) CSB, (B) CR in water on **1**.

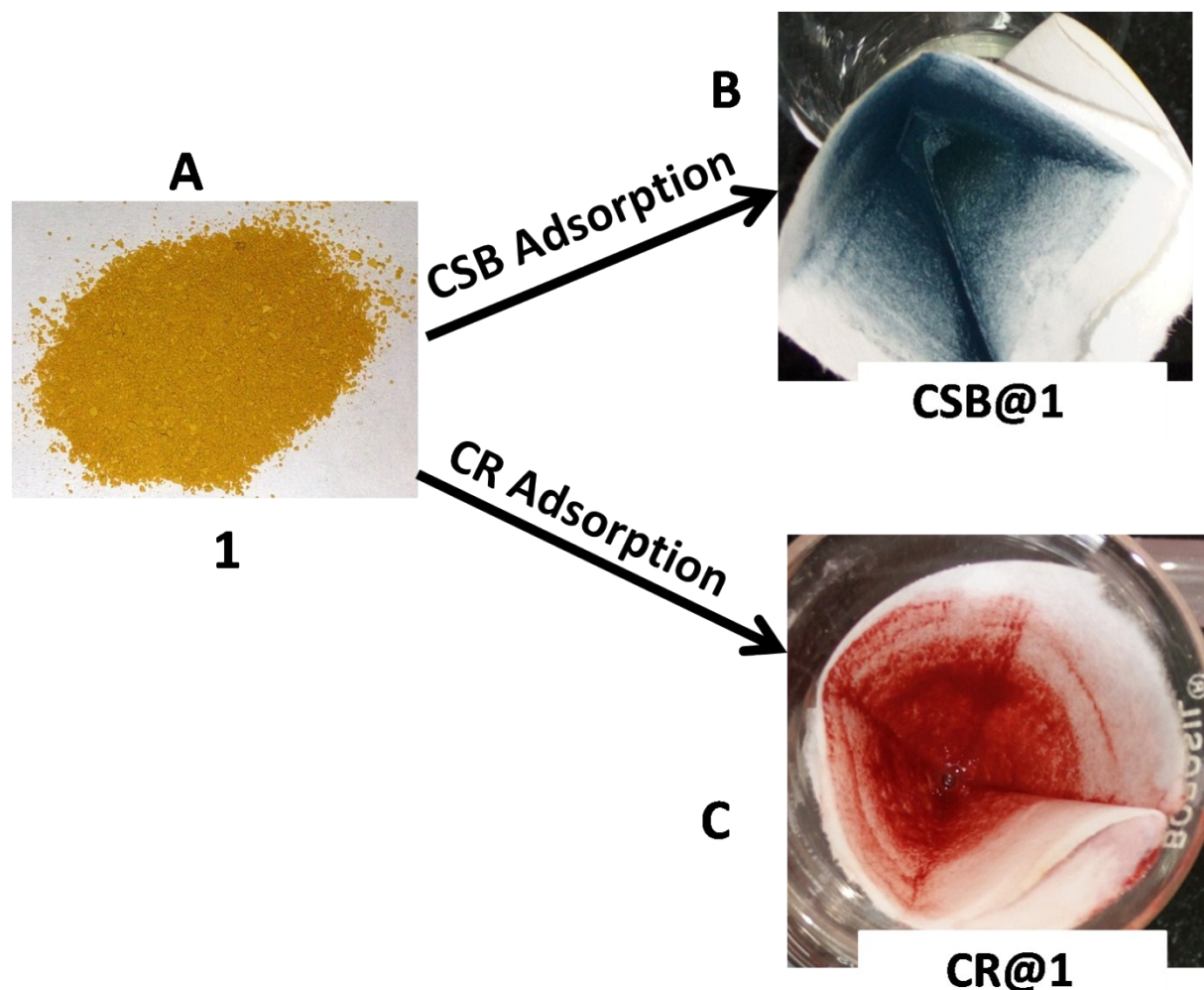


**Fig. S22** Color change of 1, (A) before adsorption, (B) after adsorption of CSB (C) after adsorption of CR.

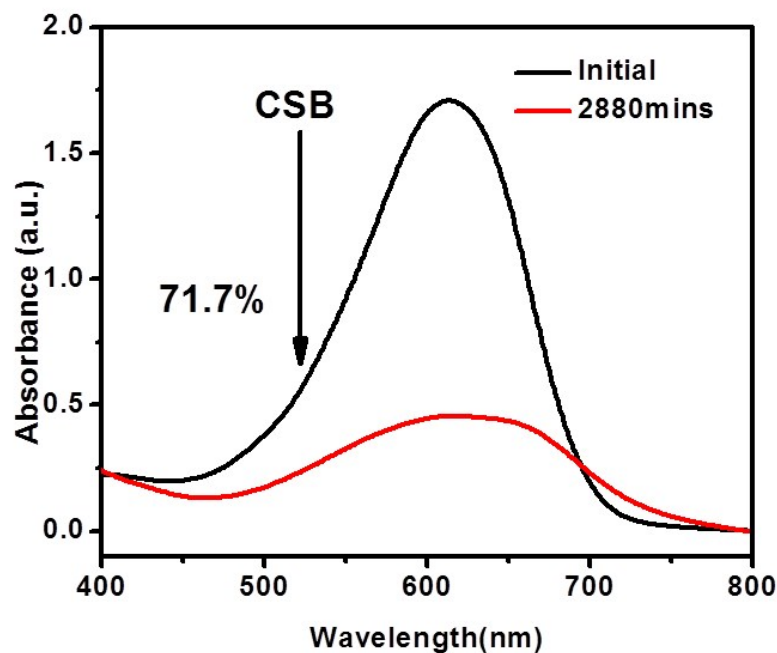


**Fig. S23** UV-vis spectra of aqueous solution of CSB adsorption by **2**.

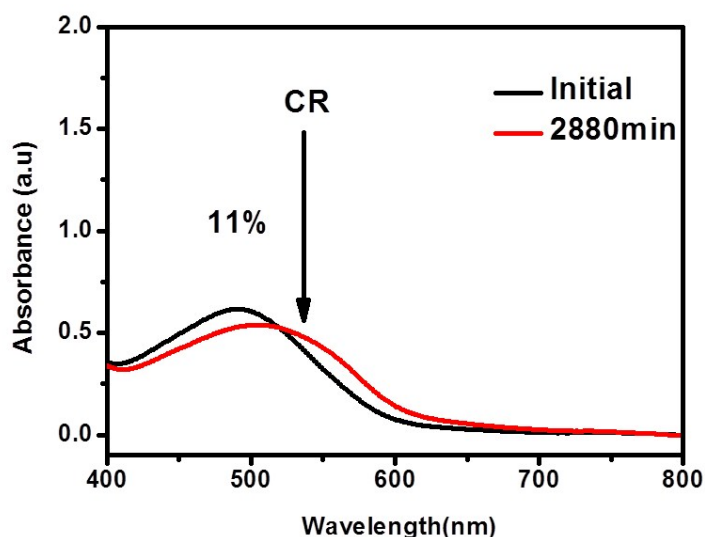


**Fig. S24** UV-vis spectra of aqueous solution of CR adsorption by **2**.

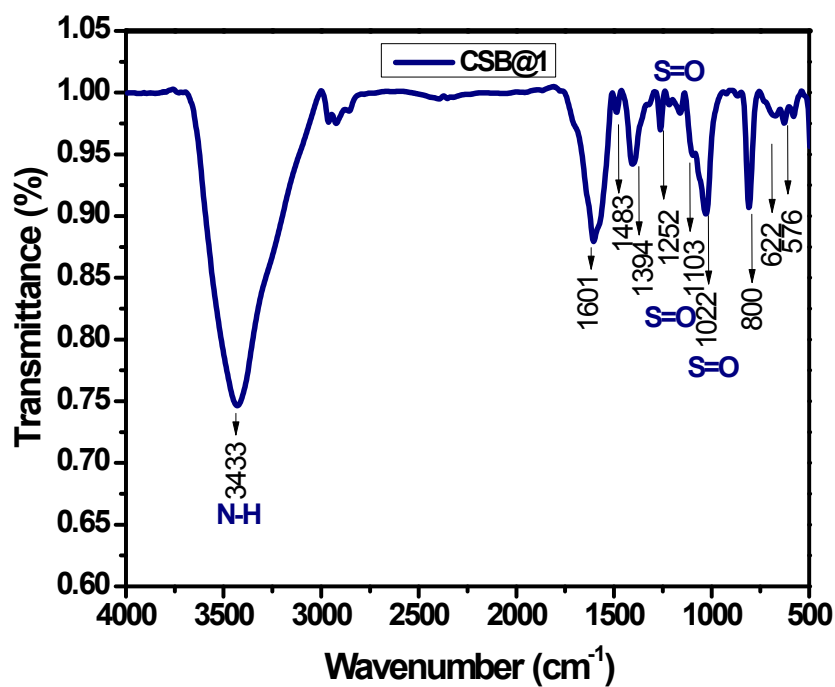


Fig. S25 FTIR analysis of CSB adsorbed on 1 (CSB@1).

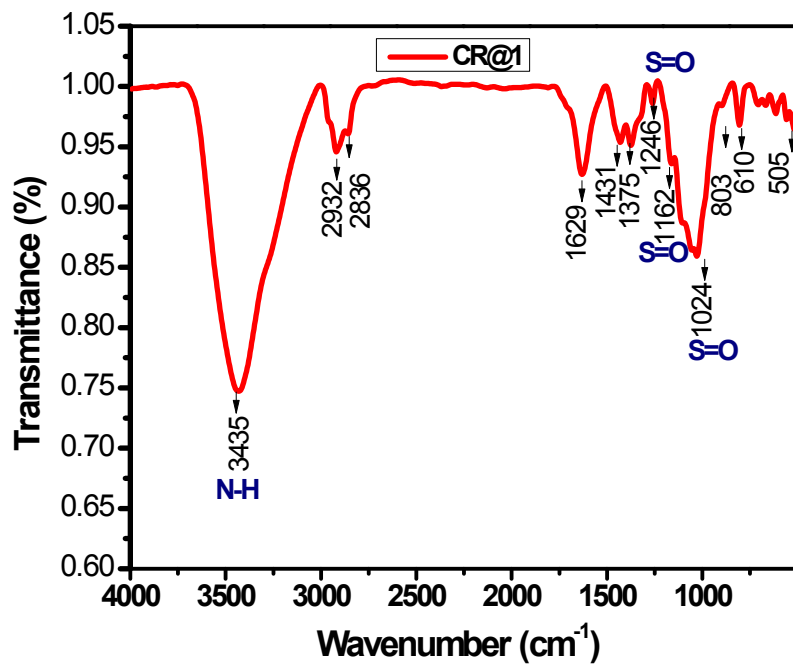
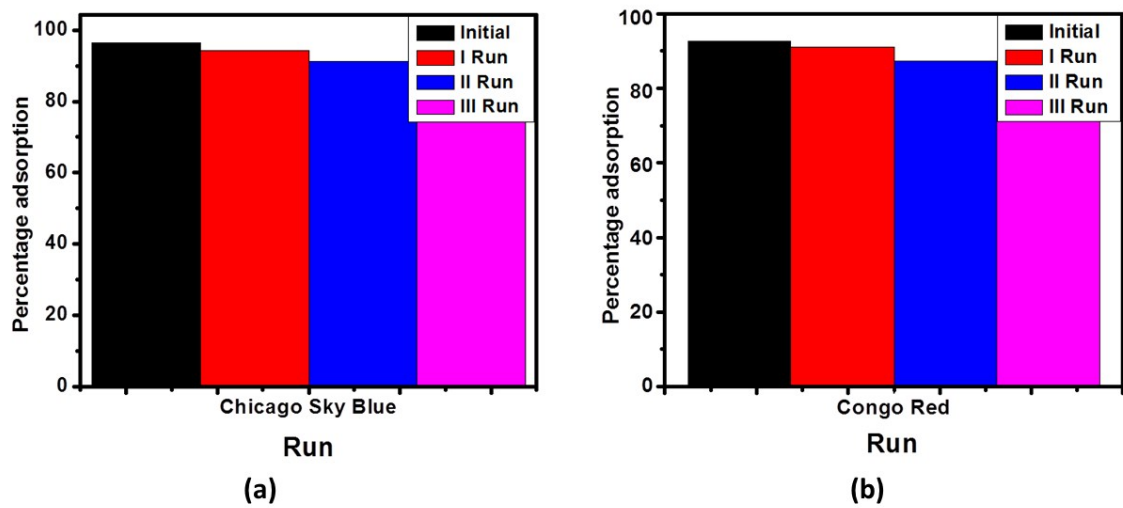


Fig. S26 FTIR analysis of CR adsorbed on 1 (CR@1).



**Fig. S27** Recyclability study of **1** towards (a) CSB and (b) CR.

### Calculation of product yield

$$\% \text{ Yield} = \frac{\text{actual number of moles}}{\text{theoretical number of moles}} \times 100\%$$

Compound	Weight (mg)	Theoretical number of moles (mmol)	Actual number of moles (mmol)	Yield (%)
1	68	0.05	0.03	60.3
2	60	0.2	0.14	72.6